

FINSLER-TYPE ESTIMATORS FOR THE CANCER CELL POPULATION DYNAMICS

Vladimir Balan and Jelena Stojanov

ABSTRACT. We introduce a Finslerian model related to the classical Garner dynamical system, which models the cancer cell population growth. The Finsler structure is determined by the energy of the deformation field—the difference of the fields, which describe the reduced and the proper biological models.

It is shown that a certain locally-Minkowski anisotropic Randers structure, obtained by means of statistical fitting, is able to provide a Zermelo-type drift of the overall cancer cell population growth, which occurs due to significant changes within the cancerous process. The geometric background, the applicative advantages and perspective openings of the constructed geometric structure are discussed.

1. The Garner cancer cell population model

It is a known fact that the subpopulations of abnormal cells responsible for the cancer disease contain the so called *cancer stem cells* (CSCs) [15]. In this context, it is very important to describe changes in the cancer population, which contains three types of cells, [11, 13]: proliferating, quiescent (resting) and dead ones, their abundance being determinant in the prognostic of the cancerous disease.

The evolution of the cancer cells population was firstly modeled in 1995 by means of Solyanik's dynamical system, which is based on the following assumptions: cancer population consists of proliferating and quiescent cells, proliferating cells can lose the division feature and transit to the quiescent ones, and quiescent cells can become proliferating or die.

The states of the Solyanik model are described by the amount \tilde{x} of proliferating cells and the amount \tilde{y} of quiescent cells, which satisfy the differential system

$$\begin{aligned}\dot{\tilde{x}} &= b\tilde{x} - P\tilde{x} + Q\tilde{y} \\ \dot{\tilde{y}} &= -d\tilde{y} + P\tilde{x} - Q\tilde{y},\end{aligned}$$

2010 *Mathematics Subject Classification*: 53B40, 37C75.

Key words and phrases: dynamical system; spherical harmonics; statistical fitting; Finsler structure; Randers metric; Holland frame.

Communicated by Stevan Pilipović.

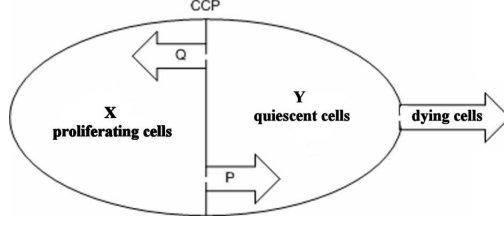


FIGURE 1. Transitions between cell classes in the Solyanik and Garner cancer evolution models

where b is the rate of cell division of the proliferating cells, d is the rate of cell death of the quiescent cells, Q and P describe the intensity of cell transition from the quiescent to proliferating cells and converse, with all the involved parameters reconsidered on a daily basis (see Fig. 1).

Solyanik's model [16] was further improved by Garner et al. in [12] by regarding the parameters P, Q as dependent on \tilde{x} and \tilde{y} , via

$$P = c(\tilde{x} + a\tilde{y}), \quad Q = \bar{A}\tilde{x}/(1 + \bar{B}\tilde{x}^2),$$

where a measures the relative nutrient uptake by resting vs. proliferating cancerous cells; c gives the magnitude of the rate of cell transition from the proliferating to the resting state; \bar{A} is the initial rate of Q increase at small \tilde{x} ; \bar{A}/\bar{B} is the rate of Q decrease for large \tilde{x} .

The Garner model describes the evolution of the scaled cell populations $x = \frac{c}{b}\tilde{x}$, $y = \frac{ca}{b}\tilde{y}$ by means of the dynamical system

$$(1.1) \quad \begin{aligned} \dot{x} &= x - x(x + y) + \frac{hxy}{1 + kx^2} \\ \dot{y} &= -ry + ax(x + y) - \frac{hxy}{1 + kx^2}, \end{aligned}$$

where $r = d/b$ is the ratio between the death rate of quiescent cells and the birth rate of proliferating cells; $h = \bar{A}/(ac)$ represents a growth factor that preferentially shifts cells from quiescent to proliferating state; $k = \bar{B} \cdot (b/c)^2$ represents a mild moderating effect.

The associated nullclines, equilibrium points, the appropriate versal deformation and the static bifurcation diagram of the Garner system were studied in [3, 4].

2. The Finsler structure and related tensor Hilbert spaces

A real Finsler structure (M, F) consists of a real n -dimensional C^∞ manifold M , and a mapping called *Finsler fundamental function* defined as follows [8, 9, 10]:

DEFINITION 2.1. A real scalar function $F : TM \rightarrow [0, \infty)$ is called a *Finsler fundamental function* if it satisfies the following properties:

- (1) F is smooth on the slit tangent space $TM \setminus \{0\} = \{(x, y) \mid x \in M, y \in T_x M, y \neq 0\}$ and is continuous on the image of the null section of the tangent bundle (TM, π, M) ;

(2) F is positively 1-homogeneous in the directional argument, i.e.,

$$F(x, \lambda y) = \lambda F(x, y), \quad \forall \lambda > 0;$$

(3) the smooth maps $g_{ij} : TM \setminus \{0\} \rightarrow \mathbb{R}$, $i, j \in \overline{1, n}$ given by

$$(2.1) \quad g_{ij} = \frac{1}{2} \frac{\partial^2 F^2}{\partial y^i \partial y^j},$$

form the symmetric positive definite matrix, $[g] = (g_{ij})_{i,j \in \overline{1, n}}$, and are the components¹ of the *Finsler metric tensor field* $g = g_{ij} dx^i \otimes dx^j$.

Also, in the case when $[g]$ is not positive definite, but non-degenerate, and with constant signature, then (M, F) is called *pseudo-Finsler structure* [5].

In our case, we shall consider extensions of this definition, by assuming that the domain of F is a strict subset of TM , and that the operations within the fibres are feasible.

A geometric object, which is specific for Finsler structures and reflects the obstruction of the Finsler metric tensor to becoming a Riemannian one is the *Cartan tensor field*, whose components are [6]

$$C_{ijk} := \frac{1}{2} \frac{\partial g_{ij}(x, y)}{\partial y^k} = \frac{1}{4} \frac{\partial^3 F^2(x, y)}{\partial y^i \partial y^j \partial y^k}.$$

Both the Finsler metric g_{ij} and the Cartan tensor field C_{ijk} , which depend on the tangent space coordinates (x, y) , belong to Hilbert spaces of (bounded and continuous) d -tensor fields of the corresponding type, $(0, 2)$ and $(0, 3)$, respectively [8, 14].

The scalar product which provides the Hilbert structure generally acts on a pair of two $(0, m)$ -tensors \mathcal{A} and \mathcal{B} by means of the formula

$$\langle \mathcal{A}, \mathcal{B} \rangle_g = \mathcal{A}_{i_1 \dots i_m} g^{i_1 j_1} \dots g^{i_m j_m} \mathcal{B}_{j_1 \dots j_m}.$$

This naturally induces the norm, the projection of \mathcal{A} onto \mathcal{B} , and the angle between the two tensors as follows:

$$\|\mathcal{A}\|_g = \sqrt{\langle \mathcal{A}, \mathcal{A} \rangle}, \quad \text{pr}_{\mathcal{B}} \mathcal{A} = \frac{\langle \mathcal{A}, \mathcal{B} \rangle}{\langle \mathcal{B}, \mathcal{B} \rangle} \mathcal{B}, \quad \sphericalangle(\mathcal{A}, \mathcal{B}) = \arccos \frac{\langle \mathcal{A}, \mathcal{B} \rangle}{\|\mathcal{A}\| \cdot \|\mathcal{B}\|}.$$

We note that all these geometric objects generally depend on the fixed Finsler metric g and on the tangent space local coordinates (x, y) .

For $m = 2$, the tensor fields are represented by square matrices A and B respectively, and for $g_{ij} = \delta_{ij}$ (i.e., Finsler space of Euclidean type), we have

$$(2.2) \quad \langle A, B \rangle_{\delta} = \text{Trace}(A \cdot B^t),$$

where $(\)^t$ is the transposition operator.

We shall further consider three types of Finsler structures: Randers, Euclidean and of 4-th root type.

¹The components g_{ij} of the fundamental metric tensor field (??) and the components g^{ij} of its dual tensor field defined by $g^{is} g_{sj} = \delta_j^i$, will be further used to lower and respectively to raise indices of tensors, for constructing geometric objects specific to the Finsler structure.

The Randers structure has the fundamental function of the form $F_R = \alpha + \beta$, where $\alpha = \sqrt{a_{ij}(x)y^i y^j}$, with the Riemannian metric $a_{ij}(x)$ and $b_i(x)$ are the coefficients of the 1-form $\beta = b_i(x)y^i$. The Euclidean structure appears as a special case, for $a_{ij} = \text{const.}$, and $b_i = 0$, $F_E = \sqrt{a_{ij}y^i y^j}$, while a 4-th root Finsler structure has the general form $F_Q = \sqrt[4]{a_{ijkl}(x)y^i y^j y^k y^l}$, where a_{ijkl} are the components of a $(0, 4)$ -tensor field on the base manifold M^2 .

We shall determine by statistical fitting over a certain model-related 2-dimensional subdomain three such metrics of the form

$$(2.3) \quad F_R(y) = \sqrt{\delta_{ij}y^i y^j + b_i y^i} = \sqrt{(y^1)^2 + (y^2)^2} + b_1 y^1 + b_2 y^2,$$

$$(2.4) \quad F_E(y) = \sqrt{c_1 \cdot (y^1)^2 + c_2 \cdot y^1 y^2 + c_3 \cdot (y^2)^2},$$

$$(2.5) \quad F_Q(y) = \sqrt[4]{q_1 \cdot (y^1)^4 + q_2 \cdot (y^1)^3 y^2 + q_3 \cdot (y^1)^2 (y^2)^2 + q_4 \cdot y^1 (y^2)^3 + q_5 \cdot (y^2)^4},$$

where the coefficients $b_{1,2}$, $c_{1,2,3}$ and $q_{1,2,3,4,5}$ are real constants providing the locally Minkowski character of the three Finsler structures. Each of the structures respectively provides the corresponding Finsler metric tensor fields: g_R , g_E and g_Q .

We shall further analyze the way these structures relate and their properties related to the model, by examining their Cartan tensors, and by estimating their shift from the associated conformally Euclidean projection.

Except for the Euclidean case (2.4), where the Cartan tensor is identically zero, the Randers and the 4-th root cases provide a nontrivial Cartan tensor, whose squared Frobenius norm is a direction-dependent scalar function provided by the transvection³ $\|C\|_g^2 = C_{ijk}g^{ir}g^{js}g^{kt}C_{rst}$.

PROPOSITION 2.1. *The following assertions hold*⁴:

- (1) *The Finsler metric produced by (2.3) has the following conformally Euclidean projection*

$$(2.6) \quad \text{pr}_\delta g_R = \frac{1}{2} \left(2 + \frac{3(b_1 \dot{x} + b_2 \dot{y})}{\sqrt{\dot{x}^2 + \dot{y}^2}} + b_1^2 + b_2^2 \right) \delta.$$

- (2) *The Finsler metric produced by (2.4) has the constant conformally Euclidean factor, i.e., the conformally flat projection is*

$$(2.7) \quad \text{pr}_\delta g_E = \frac{1}{2}(c_1 + c_3)\delta.$$

- (3) *The Finsler metric produced by (2.5) has the following conformally Euclidean projection*

$$(2.8) \quad \text{pr}_\delta g_Q = \frac{p}{16F_Q^6}\delta,$$

²We assume F_Q defined on the subdomain of TM which ensures the positivity of the root argument; as well, we note that F_Q is a pseudo-Finsler norm, whose smoothness is ensured on a strict subdomain of the slit tangent space.

³In [10], an alternative of norm for the Cartan tensor is presented, which results in a numerical value.

⁴Hereby we denote by δ the canonic metric for the Euclidean 2-dimensional case, and use the notation $\mathbf{y} = (y^1, y^2) = (\dot{x}, \dot{y})$.

where p is the following polynomial in the components of the tangent vector $\mathbf{y} = (y^1, y^2) = (\dot{x}, \dot{y})$:

$$(2.9) \quad \begin{aligned} p = & (8q_1^2 + 4q_1q_3 - q_2^2)\dot{x}^6 + (12q_1q_4 + 12q_1q_2)\dot{x}^5\dot{y} \\ & + (12q_1q_3 + 6q_2q_4 + 24q_1q_5 + 3q_2^2)\dot{x}^4\dot{y}^2 \\ & + (16q_1q_4 + 4q_2q_3 + 16q_2q_5 + 4q_3q_4)\dot{x}^3\dot{y}^3 \\ & + (12q_3q_5 + 3q_4^2 + 24q_1q_5 + 6q_2q_4)\dot{x}^2\dot{y}^4 \\ & + (12q_4q_5 + 12q_2q_5)\dot{x}\dot{y}^5 + (4q_3q_5 + 8q_5^2 - q_4^2)\dot{y}^6. \end{aligned}$$

PROOF. A straightforward calculation produces the components of Finsler metric tensor fields in the all three cases:

$$\begin{aligned} g_{R11} &= -\frac{\beta}{\alpha^3}\dot{x}^2 + \frac{2}{\alpha}b_1\dot{x} + \frac{F}{\alpha} + b_1^2, \\ g_{R12} &= -\frac{\beta}{\alpha^3}\dot{x}\dot{y} + \frac{b_2}{\alpha}\dot{x} + \frac{b_1}{\alpha}\dot{y} + b_1b_2, \\ g_{R22} &= -\frac{\beta}{\alpha^3}\dot{y}^2 + \frac{2}{\alpha}b_2\dot{y} + \frac{F}{\alpha} + b_2^2; \\ g_{E11} &= c_1, \quad g_{E12} = \frac{1}{2}c_2, \quad g_{E22} = c_3; \end{aligned}$$

$$\begin{aligned} g_{Q11} &= \frac{1}{8F^6} (8q_1^2\dot{x}^6 + 12q_1q_2\dot{x}^5\dot{y} + (3q_2^2 + 12q_1q_3)\dot{x}^4\dot{y}^2 \\ & + (4q_2q_3 + 16q_1q_4)\dot{x}^3\dot{y}^3 + (24q_1q_5 + 6q_2q_4)\dot{x}^2\dot{y}^4 \\ & + 12q_2q_5\dot{x}\dot{y}^5 + (4q_3q_5 - q_4^2)\dot{y}^6) \end{aligned}$$

$$\begin{aligned} g_{Q12} &= \frac{1}{8F^6} (2q_1q_2\dot{x}^6 + 3q_2^2\dot{x}^5\dot{y} + 6(q_2q_3 - q_1q_4)\dot{x}^4\dot{y}^2 + (2q_2q_4 + 4q_3^2 - 16q_1q_5)\dot{x}^3\dot{y}^3 \\ & + 6(q_3q_4 - q_2q_5)\dot{x}^2\dot{y}^4 + 3q_4^2\dot{x}\dot{y}^5 + 2q_4q_5\dot{y}^6) \end{aligned}$$

$$\begin{aligned} g_{Q22} &= \frac{1}{8F^6} ((4q_1q_3 - q_2^2)\dot{x}^6 + 12q_1q_4\dot{x}^5\dot{y} + (24q_1q_5 + 6q_2q_4)\dot{x}^4\dot{y}^2 \\ & + (16q_2q_5 + 4q_3q_4)\dot{x}^3\dot{y}^3 + (12q_3q_5 + 3q_4^2)\dot{x}^2\dot{y}^4 + 12q_4q_5\dot{x}\dot{y}^5 + 8q_5^2\dot{y}^6). \end{aligned}$$

Inner product (2.2) of g and δ reduces to the trace and $\langle \delta, \delta \rangle = 2$, hence summation $\frac{1}{2}(g_{11} + g_{22})$ gives the conformal factors at (2.6), (2.7) and (2.8). \square

PROPOSITION 2.2. *In the Hilbert space of $(0, 2)$ -type Finsler tensors, the following deviation angles occur:*

- (1) *The Finsler-Randers metric produced by (2.3) deviates from its conformally Euclidean approximation by the angle*

$$(2.10) \quad \theta_R = \arccos \sqrt{\frac{1}{2} + \frac{(A+1)(A^2 - 4A + 1)}{(2 + 3A + B)^2 - 2(A+1)(A^2 - 4A + 1)}},$$

where the following abbreviations are used: $A = (b_1\dot{x} + b_2\dot{y})/\sqrt{\dot{x}^2 + \dot{y}^2}$ and $B = b_1^2 + b_2^2$.

- (2) *The Finsler metric produced by (2.4) and its conformally flat approximation determine the constant deviation angle*

$$\theta_E = \arccos \frac{c_1 + c_3}{\sqrt{2c_1^2 + c_2^2 + 2c_3^2}}.$$

- (3) *The deviation function expressing the angle between the Finsler metric produced by (2.5) and its conformally Euclidean approximation is*

$$(2.11) \quad \theta_Q = \arccos \frac{p}{\sqrt{2s}},$$

where p is the polynomial from (2.9), and $s = \pi + \sigma(\pi)$ is a polynomial in \dot{x}, \dot{y} with

$$\begin{aligned} \pi = & \left(64q_1^4 + 8q_1^2q_2^2 - 8q_1q_2^2q_3 + 16q_1^2q_3^2 + q_2^4\right)\dot{x}^{12} \\ & + \left(192q_1^3q_2 + 96q_1^2q_3q_4 - 24q_1q_2^2q_4 + 24q_1q_2^3\right)\dot{x}^{11}\dot{y} \\ & + \left(192q_1^3q_3 + 192q_1^2q_2^2 + 144q_1^2q_4^2 - 48q_1^2q_2q_4 + 192q_1^2q_3q_5 \right. \\ & \quad \left. + 48q_1q_2q_3q_4 + 48q_1q_2^2q_3 - 48q_1q_2^2q_5 - 12q_2^3q_4 + 18q_2^4\right)\dot{x}^{10}\dot{y}^2 \\ & + \left(256q_1^3q_4 + 352q_1^2q_2q_3 - 128q_1^2q_2q_5 + 576q_1^2q_4q_5 + 128q_1q_2q_3q_5 \right. \\ & \quad \left. - 56q_1q_2^2q_4 + 32q_1q_2q_3^2 + 144q_1q_2q_4^2 - 8q_2^2q_4q_3 \right. \\ & \quad \left. + 32q_1q_4q_3^2 + 72q_1q_2^3 + 72q_2^3q_3 - 32q_2^3q_5\right)\dot{x}^9\dot{y}^3 \\ & + \left(384q_1^3q_5 + 144q_1^2q_3^2 + 72q_1^2q_4^2 + 576q_1^2q_5^2 + 480q_1^2q_2q_4 - 96q_1q_2q_4q_3 \right. \\ & \quad \left. + 672q_1q_2q_4q_5 + 168q_1q_2^2q_3 + 96q_1q_3^2q_5 + 120q_1q_3q_4^2 \right. \\ & \quad \left. + 30q_2^2q_4^2 - 240q_1q_2^2q_5 - 24q_2^2q_3q_5 + 120q_2^2q_3^2 + 24q_2^3q_4 + 9q_2^4\right)\dot{x}^8\dot{y}^4 \\ & + \left(768q_1^2q_2q_5 + 384q_1^2q_3q_4 + 384q_1^2q_4q_5 - 96q_1q_3^2q_4 + 768q_1q_2q_5^2 - 384q_1q_2q_3q_5 \right. \\ & \quad \left. + 576q_1q_3q_4q_5 + 48q_2q_3q_4^2 - 72q_2^3q_5 + 168q_2^2q_4q_5 + 120q_2^2q_3q_4 + 240q_1q_2^2q_4 \right. \\ & \quad \left. - 24q_1q_2q_4^2 + 96q_1q_2q_3^2 + 72q_1q_4^3 + 24q_2^3q_3 + 96q_2q_3^3\right)\dot{x}^7\dot{y}^5 \\ & + \left(512q_1^2q_5^2 + 640q_1^2q_3q_5 + 272q_1q_2q_3q_4 + 32q_1q_2q_4q_5 + 272q_2q_3q_4q_5 \right. \\ & \quad \left. + 432q_1q_2^2q_5 - 144q_1q_3q_4^2 - 144q_2^2q_3q_5 - 256q_1q_3^2q_5 + 432q_1q_4^2q_5 \right. \\ & \quad \left. + 44q_2^2q_4^2 + 640q_1q_3q_5^2 + 176q_2q_3^2q_4 + 240q_1^2q_4^2 + 16q_2^2q_3^2 \right. \\ & \quad \left. + 16q_3^2q_4^2 + 240q_2^2q_5^2 + 36q_2^3q_4 + 36q_2q_4^3 + 32q_3^4\right)\dot{x}^6\dot{y}^6 \cdot \frac{1}{2}, \end{aligned}$$

and $\sigma(\pi)$ produced from π after interchanging

$$(q_1, q_2, q_3, q_4, q_5, \dot{x}, \dot{y}) \leftrightarrow (q_5, q_4, q_3, q_2, q_1, \dot{y}, \dot{x}).$$

PROOF. Let f be the conformal Euclidean factor of the projection in the equations (2.6)–(2.8), and let $\theta = \sphericalangle(g, \text{pr}_\delta g)$ be the angle between the corresponding metric and its projection to δ . Then, the homogeneity of the inner product implies

$$\cos \theta = \frac{\langle g, f\delta \rangle}{\sqrt{\langle g, g \rangle} \sqrt{f^2 \langle \delta, \delta \rangle}} = \text{sign}(f) \cdot \frac{\langle g, \delta \rangle}{\sqrt{\langle g, g \rangle} \sqrt{\langle \delta, \delta \rangle}} = \text{sign}(f) \cdot \cos \sphericalangle(g, \delta).$$

By use of (2.2), we have the following expressions⁵

$$\cos \theta = \frac{g_{11} + g_{22}}{\sqrt{2(g_{11}^2 + 2g_{12}^2 + g_{22}^2)}}, \quad \sphericalangle(g, \delta) = \arccos \sqrt{\frac{(g_{11} + g_{22})^2}{2(g_{11}^2 + 2g_{12}^2 + g_{22}^2)}}.$$

By plugging into the previous formula the appropriate metric components, one gets (2.10)–(2.11). \square

The proposed Finsler functions are of locally Minkowski type, which infers that many geometric objects related to them considerably simplify: the geodesics are (pieces of) straight lines, the KCC invariants vanish, the Berwald linear connection is trivial [1, 8]. In fact, the Finsler structures will provide point-independent norms, which act on a certain proper subset of the space $TM = T\mathbb{R}^2$.

3. The statistic fitting of the Finsler structures

3.1. The reduced Garner system. We observe that the original Garner dynamical system (1.1), denoted further as GS , is the extended version of the reduced dynamical system (denoted as RS)⁶:

$$(3.1) \quad \begin{aligned} \dot{x} &= x - x(x + y) \\ \dot{y} &= -ry + ax(x + y). \end{aligned}$$

We note that in the original system GS , for h being significant one notices a malignant evolution of the illness; this happens when:

- the parameter a significantly decreases, becoming negligible (i.e., there is a small ratio of nutrient uptake of resting vs. proliferating cells, which shows that the resources are absorbed mostly by the proliferating cells in detriment of quiescent cells);
- the parameter c is negligible (i.e., the rate of cell transition from cancerous to the resting state is negligible, hence the evolution of the disease is either stationary, or worsening);
- the parameter \bar{A} significantly increases (the rate of increase of Q is abruptly big at small x , i.e., the cell transition from the quiescent to cancerous cells is intense).

We conclude that when these conditions are far from being achieved (this might happen, e.g., under treatment, which may significantly modify the intake of nutrient ratio in disfavor of cancerous cells), the GS (1.1) can be approximated by RS (3.1).

⁵We shall further consider the absolute value of the factor, reducing thus the angle to the first quadrant.

⁶This occurs when in system (3.1) the constant $h = \bar{A}/(ac)$ is negligible, $0 < |h| \ll 1$.

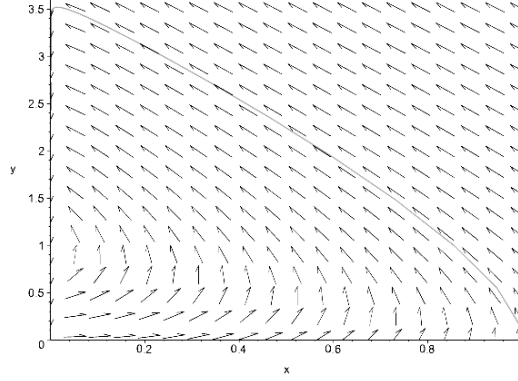


FIGURE 2. The field lines of the reduced Garner model RS , for $a = 1.998958904$ and $r = 0.03$.

3.2. The increase rate of cancer cell populations for mild premises.

As described in the previous section, under mild (controlled) evolution of the disease (for $0 \leq |h| \ll 1$), the RS system (3.1) reasonably approximates the original system (1.1).

The set of all possible states of the Garner's dynamical system is a bounded subset D of the first quadrant in \mathbb{R}^2 , $K_+ = \{p = (x, y) \mid x > 0, y > 0\}$, which contains the information on the scaled amount of proliferating and of quiescent cells.

The RS (3.1) attaches to any point $p = (x, y) \in D$ its related velocity $\dot{p} = (\dot{x}, \dot{y}) \in T_{(x,y)}(K_+)$. Due to the polynomial form of the vector field, RS provides a reverse association $\dot{p} = (\dot{x}, \dot{y}) \rightsquigarrow p(x, y)$, by solving the nonlinear algebraic system (3.1) in terms of $p = (x, y)$ for given $\dot{p} = (\dot{x}, \dot{y})$, but only in certain regions of K_+ and only for certain values of the parameters r, h, k .

We shall further consider the RS system for the case of fixed parameters [12]:

$$(A1) \quad a = 1.998958904 \text{ and } r = 0.03.$$

We choose the domain D of the Finsler norm F as a set of tangent vectors, where $D = \varphi(I_\rho \times I_\theta) \subset T_p K_+$, with

$$I_\rho \times I_\theta = [0.329915, 0.888939] \times [1.0988, 1.51452] \subset [0, \infty) \times [0, 2\pi),$$

and φ is the mapping which changes the polar coordinates to the Cartesian ones,

$$\varphi : [0, \infty) \times [0, 2\pi) \rightarrow \mathbb{R}^2, \quad \varphi(\rho, \theta) = (\rho \cos \theta, \rho \sin \theta).$$

Under an appropriate choice of I_1 and I_2 , one can uniquely solve the quadratic system (3.1) in terms of $p = (x, y)$, with P located on a field line from K_+ , with related tangent direction of the emerging velocity $\dot{p} \in D$.

By using the inverse function theorem for the feasible directions of the reduced dynamical system, one may solve the pair of algebraic nonlinear equations of the system, to locally find the associated point p .

3.3. The rate-shift under changes of premises. The status of the cancerous disease changes from mild to severe status due to a multitude of factors which corresponds to a change of parameters in the *GS* Garner system (1.1).

Such a case occurs when h becomes significant; this transforms *RS* into *GS* and then (1.1) associates to the solutions p from the nonlinear system, the new rates of change $\dot{p}_e = (\dot{x}_e, \dot{x}_e)$ valid for the new circumstances of the illness. Namely, the point coordinates $p = (x, y)$ determined under mild conditions in Subsection 3.2, plugging in (1.1), produce the new change rate \dot{p}_e of the cancer cell populations (see Fig. 3).

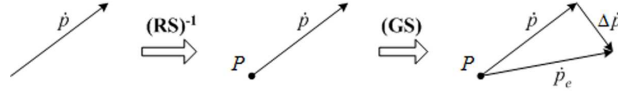


FIGURE 3. The transition $\dot{p} \rightsquigarrow \dot{p}_e$ between the *RS* and the *GS* change rates.

3.4. Statistical fitting of the Finsler norms. The Euclidean norm $\|\dot{p}_e\|_E$ of the obtained rate-vector $\dot{p}_e = (\dot{x}_e, \dot{x}_e)$ can be used to evaluate the severeness of the disease evolution. This choice, however, has the drawback of being symmetric in the two components of \dot{p}_e , especially in the case $\dot{x} > 0$, since equal credit is given to the two rates of the increase.

One alternative choice is to design a tool which emphasizes the cancer cell population increase, by means of a *Finsler norm*, which is likely to emphasize a tuned fair evaluation of the illness evolution.

To this aim we note that $\|\dot{p}_e\|$ can provide locally Minkowski (i.e., depending on directional variables only) Finsler norms $F_R(\dot{x}, \dot{y})$, $F_E(\dot{x}, \dot{y})$ and $F_Q(\dot{x}, \dot{y})$ by statistical fitting⁷.

The proposed approximation, which provides the fit of the Finsler norm F is given by

$$(3.2) \quad F(\dot{x}, \dot{y}) \sim \|\dot{p}_e\|_E,$$

where $\|\cdot\|_E$ is the Euclidean norm. We note that the triangle inequality for norms shows that the rate-jump entailed by the change of status $RS \rightarrow GS$ due to the increase of $|h|$, does not exceed $\|\dot{p}_e - \dot{p}\|_E$.

We shall consider the following choices which follow the main requirements of a Finsler norm, and which are fundamental functions of locally Minkowski type⁸:

$$(3.3) \quad F_R(\dot{x}, \dot{y}) = \sqrt{\dot{x}^2 + \dot{y}^2} + b_1\dot{x} + b_2\dot{y}$$

$$(3.4) \quad F_E(\dot{x}, \dot{y}) = \sqrt{c_1\dot{x}^2 + c_2\dot{x}\dot{y} + c_3\dot{y}^2}$$

$$(3.5) \quad F_Q(\dot{x}, \dot{y}) = \sqrt[4]{a(\dot{x})^4 + b(\dot{x})^3(\dot{y}) + c(\dot{x})^2(\dot{y})^2 + d(\dot{x})(\dot{y})^3 + e(\dot{y})^4}$$

⁷Generally, when considering one of the three structures, we shall simply write $F(\dot{x}, \dot{y})$. Similar procedures of Finslerian statistical fitting were performed in [2].

⁸For brevity, we denote $(a, b, c, d, e) := (q_1, q_2, q_3, q_4, q_5)$.

where $b_{1,2}$ and $c_{1,2,3}$ and $(a, b, c, d, e) = (q_1, q_2, q_3, q_4, q_5)$ are coefficients to be evaluated by statistic fitting.

In our research, we use the values assumed in (A1) for the systems *RS* (3.1) and *GS* (1.1).

For the statistical fitting of $F(\dot{p})$ from (3.2) to $\|\dot{p}_e\|$, where $\dot{p} = (\dot{x}, \dot{y})$, and $p = (x, y)$, $\dot{p}_e = (\dot{x}_e, \dot{y}_e)$ are respectively obtained by tracing the process described in Fig. 3, we use for the Randers, Euclidean and 4-th root cases the following equalities ($k \in \overline{1, N}$)

$$(3.6) \quad b_1 \dot{x}_k + b_2 \dot{y}_k = \sqrt{(\dot{x}_e)_k^2 + (\dot{y}_e)_k^2} - \sqrt{\dot{x}_k^2 + \dot{y}_k^2},$$

$$(3.7) \quad c_1 \dot{x}_k^2 + c_2 \dot{x}_k \dot{y}_k + c_3 \dot{y}_k^2 = (\dot{x}_e)_k^2 + (\dot{y}_e)_k^2,$$

$$(3.8) \quad a(\dot{x}_k)^4 + b(\dot{x}_k)^3(\dot{y}_k) + c(\dot{x}_k)^2(\dot{y}_k)^2 + d(\dot{x}_k)(\dot{y}_k)^3 + e(\dot{y}_k)^4 = ((\dot{x}_e)_k^2 + (\dot{y}_e)_k^2)^2,$$

which allows us to determine the statistical fit for the values $b_{1,2}$, $c_{1,2,3}$ and a, b, c, d, e by the method of least squares.

For finding \dot{p}_e from \dot{p} via *RS* and further *GS*, we use in (1.1) the parameter values [3, 12]

$$(A2) \quad h = 1.236 \text{ and } k = 0.236.$$

As inputs for the fitting process, we employ a uniform grid over the (ρ, θ) -domain $I_\rho \times I_\theta = [0.329915, 0.888939] \times [1.0988, 1.51452]$,

$$(\rho_i, \theta_j) \in I_\rho \times I_\theta, (i, j) \in \overline{0, n_\rho} \times \overline{0, n_\theta},$$

with $\varphi(I_\rho \times I_\theta) = I_1 \times I_2 = [0.05, 0.1596] \times [0.293844, 0.887532]$, and consider as related tangent vectors the following scaled spherical harmonics

$$\dot{p}_k = (\dot{x}_k, \dot{y}_k) = (\rho_i \cos \theta_j, \rho_i \sin \theta_j) \in D = I_1 \times I_2, \quad k \in \overline{1, N}$$

where $k = (i - 1)n_\rho + j \in \overline{1, N}$, and $N = (n_\rho + 1)(n_\theta + 1)$.

We note that the right hand side of the *RS* contains quadratic polynomials, and that for given input $\dot{p} = \dot{p}_1$, $(RS)^{-1}$ provides a twofold point-solution, p', p'' , of which one solution p_1 is chosen.

For each next plugged-in scaled spherical harmonic \dot{p}_{k+1} , *RS* similarly provides two other point-solutions, and the right choice p_{k+1} is determined by both the non-negativity of its components and by the Euclidean proximity to the previous selected point p_k ($k \in \overline{1, N-1}$).

Finally, one gets the set of points $p_k = (x_k, y_k)$ and (via *GS*) the corresponding change rates $(\dot{p}_e)_k$, $k \in \overline{1, N}$, which are further plugged in (3.6)-(3.8).

The N samples \dot{p}_k and the new rates $(\dot{p}_e)_k$ ($k \in \overline{1, N}$), plugged in the N relations from (3.6)-(3.8), provide in each case N linear equations with parameters as unknowns which fix the Finsler function (3.3)-(3.5).

3.4.1. The Randers fitting. The system (3.6) is linear relative to b_1 and b_2 , over-determined ($N \gg 2$), and has the form $AS = B$, where $A = (\dot{x}_k, \dot{y}_k)_{k \in \overline{1, N}} \in M_{N \times 2}(\mathbb{R})$, $S = (b_1, b_2)^t \in M_{2 \times 1}(\mathbb{R})$ is the unknown vector, and $B \in M_{N \times 1}(\mathbb{R})$ is given by the r.h.s. of (3.6) for $k \in \overline{1, N}$.

Computer Maple 17 simulation for $N = 36$, provides by the least square method the pseudosolution $(b_1, b_2)^t = (A^t A)^{-1} A^t B$, and under assumptions (A1) and (A2), the exact fit-values of the parameters are

$$(3.9) \quad b_1 \approx 0.628481987778205518, \quad b_2 \approx -0.269476980932055964.$$

Hence the fit Randers structure related to the dynamical system of the Garner cancer cells population model (1.1) becomes (for the obtained (3.9) fit values of the parameters)

$$(3.10) \quad F_R(\dot{x}, \dot{y}) \approx \sqrt{\dot{x}^2 + \dot{y}^2} + 0.63 \cdot \dot{x} - 0.27 \cdot \dot{y}$$

where the dot marks denote time derivatives, which describe the rates of increase for the scaled cancer cell populations⁹.

3.4.2. *The Euclidean fitting.* For the Euclidean case, for fixing the Finsler function (3.4), the same N samples \dot{p}_k and new rates $(\dot{p}_e)_k$ ($k = 1, N$), are plugged in the N relations (3.7).

The obtained system is linear in terms of c_1 , c_2 and c_3 , superdetermined ($N \gg 3$), and has the form $AS = B$, where $A \in M_{N \times 3}(\mathbb{R})$, $S \in M_{3 \times 1}(\mathbb{R})$, and $B \in M_{N \times 1}(\mathbb{R})$, with the unknown vector $S = (c_1, c_2, c_3)^t$.

Analogous computer simulation provides the parameters solution

$$\begin{aligned} c_1 &\approx 0.940805450748692151 \\ c_2 &\approx 1.16189809024084268 \\ c_3 &\approx 0.496069555231253400, \end{aligned}$$

hence the Euclidean type fundamental function of the structure fit to (1.1), is

$$F_E(\dot{x}, \dot{y}) \approx \sqrt{0.94\dot{x}^2 + 1.16\dot{x}\dot{y} + 0.50\dot{y}^2}.$$

3.4.3. *The 4-th root fitting.* The 4-th root type Finsler function (3.5) (the third case) is determined by use of the same method as in the previous two cases with the differences: $A \in M_{N \times 5}(\mathbb{R})$, $S \in M_{5 \times 1}(\mathbb{R})$, and $S = (a, b, c, d, e)^t$.

The same computer simulation provides the parameters solution¹⁰:

$$(3.11) \quad \begin{aligned} a &\approx -0.320013354328217758; & b &\approx 2.69642032805366582; \\ c &\approx 2.42492765757201711; & d &\approx 1.07381846633249766; \\ e &\approx 0.254991915496320776, \end{aligned}$$

hence the fit 4-th root Finsler fundamental function locally related to the GS (1.1) is

$$(3.12) \quad F_Q(\dot{x}, \dot{y}) \approx \sqrt[4]{-0.32\dot{x}^4 + 2.70\dot{x}^3\dot{y} + 2.42\dot{x}^2\dot{y}^2 + 1.07\dot{x}\dot{y}^3 + 0.25\dot{y}^4}.$$

⁹For display convenience, truncated values of the coefficients have been used, in this, but also in the next two structures

¹⁰For brevity, we denote $(a, b, c, d, e) := (q_1, q_2, q_3, q_4, q_5)$.

4. The properties of the constructed Finsler metric structures

4.1. The Randers type structure. Regarding the Randers structure, it is remarkable that for $\|b\|_g < 1$, which is our case, one has (g_{ij}) positive definite, and there exists a vertical non-holonomic frame

$$\mathcal{F}_H = \left\{ X_j \mid X_j = X_j^i \frac{\partial}{\partial y^i}, \quad j = \overline{1, 2} \right\},$$

called *the Holland frame* of the Randers structure [8],

$$X_j^i = \sqrt{\alpha/F} \left(\delta_j^i - \frac{y^i(\alpha_j + b_j)}{F} + \sqrt{\alpha/F} \cdot \frac{y^i \alpha_j}{\alpha} \right), \quad j = \overline{1, 2},$$

in which the Randers metric tensor field g_{ij} becomes the α -subjacent Riemannian one and $\alpha_i = \frac{\partial \alpha}{\partial y^i} = \frac{y^i}{\alpha}$. In this respect, we get the following results.

PROPOSITION 4.1. *The following assertions hold true:*

a) *The associated Finsler metric tensor field $g = g_{ij}(\dot{p}) dx^i \otimes dx^j$ of the Randers structure F_R has the components*

$$(4.1) \quad g_{ij}(y) = \frac{\alpha + \beta}{\alpha} \left(\delta_{ij} - \frac{y^i y^j}{\alpha^2} \right) + \frac{y^i y^j + \alpha(b_i y^j + b_j y^i) + b_i b_j \alpha^2}{\alpha^2},$$

where $\mathbf{y} = (y^1, y^2) = (\dot{x}, \dot{y})$, $b_1 \approx 0.63$, $b_2 \approx -0.27$ and¹¹

$$\alpha = \sqrt{\delta_{ij} y^i y^j} = \sqrt{\dot{x}^2 + \dot{y}^2}, \quad \beta = b_i y^i = b_1 \dot{x} + b_2 \dot{y}.$$

b) *For the Finsler structure (3.3), the components of the fields of the Holland frame are given by*

$$X_j^i = \frac{\alpha F \delta_j^i - y^i (y^j + \alpha b_j)}{\sqrt{\alpha F^3}} + \frac{y^i y^j}{\alpha F}, \quad j = \overline{1, 2}.$$

PROOF. a) By a direct computation, one obtains

$$\begin{aligned} g_{ij}(y) &= \frac{F}{\alpha} (\delta_{ij} - \alpha_i \alpha_j) + (\alpha_i + b_i)(\alpha_j + b_j) \\ &= \frac{\alpha + \beta}{\alpha} \left(\delta_{ij} - \frac{1}{\alpha^2} y^i y^j \right) + \left(\frac{y^i}{\alpha} + b_i \right) \left(\frac{y^j}{\alpha} + b_j \right), \end{aligned}$$

whence result (4.1) follows. For b), one notices that using the definition of the Holland frame [8] and, by performing the calculations for our locally-Minkowski particular norm, one infers the claimed result. \square

Moreover, by plugging in the fit coefficients from (3.10) into the appropriate equations from Propositions 2.1 and 2.2 one gets the following

¹¹For display convenience, truncated values of the coefficients have been used, of the more accurate statistically determined values $b_1 = 0.62848198778205518 \cdot r \cdot \cos(t)$ and $b_2 = -0.269476980932055964 \cdot r \cdot \sin(t)$.

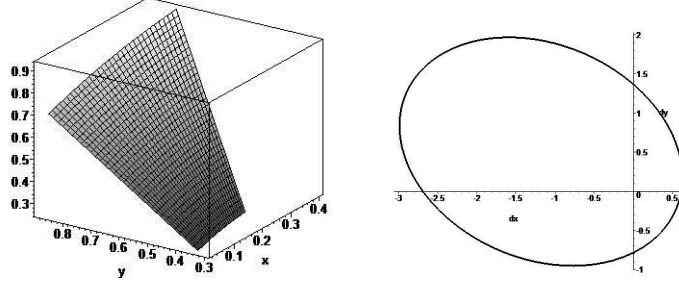


FIGURE 4. Plot of the squared locally Minkowski Finsler Randers norm $z = F^2(\dot{x}, \dot{y})$ and of the indicatrix $F(\dot{x}, \dot{y}) = 1$

COROLLARY 4.1. *The conformally Euclidean projection of the metric produced by the Randers type Finsler structure (3.10) is*

$$\text{pr}_\delta g_R \approx \left(\frac{0.945\dot{x} - 0.405\dot{y}}{\sqrt{\dot{x}^2 + \dot{y}^2}} + 1.235 \right) \delta,$$

and the deviation between these two metrics is given by

$$\theta_R \approx \arccos \frac{1.89\alpha\dot{x} - 0.81\alpha\dot{y} + 2.47\alpha^2}{\sqrt{r}},$$

where $\alpha = \sqrt{\dot{x}^2 + \dot{y}^2}$ and

$$r = -4.68\alpha^3\dot{y} + 1.20\alpha\dot{x}^2\dot{y} - 0.44\alpha\dot{x}^3 + 10.56\alpha^3\dot{x} + 8.64\alpha^4 + 1.94\alpha^2\dot{x}^2 - 2.04\alpha^2\dot{x}\dot{y}.$$

The graphical representation of the values of the Finsler-Randers norm along the z -axis in terms of the inputs $(\dot{x}, \dot{y}) \in D = [0.05, 0.1596] \times [0.293844, 0.887532]$, and of the Finsler indicatrix are provided in Fig. 4. These clearly exhibit convexity and compactness of the Randers indicatrix of (3.10).

By Maple symbolic programming one can easily test that the signature of the metric g is $(+, +)$, hence (D, F) with $D \subset K_+$ is a Randers geometric structure of locally-Minkowski type [14].

To illustrate the signature of the point-independent metric tensor g , one can see that, within a fiber of $T_{\dot{p}}\mathbb{R}^2$, its associated quadratic form¹²

$$Q_{\mathbf{y}}^g(v) = g_{ij}|_{\mathbf{y}} v^i v^j, \quad v = (v^i, v^j) \in \mathbb{R}^2 \equiv T_{\dot{p}}\mathbb{R}^2$$

has its graph an elliptic paraboloid patch (see Fig. 5), which gives account of the positive signature of g , signalled by the inequality $\|b\|^2 \equiv b_1^2 + b_2^2 \approx 0.63^2 + 0.27^2 < 1$.

We note as well that the Cartan tensor $C_{ijk} = \frac{1}{4} \frac{\partial^3 F^2}{\partial y^i \partial y^j \partial y^k}$ measures the “distance” between the constructed Finslerian F norm and the space of flat Euclidean-type norms. The distance can be locally estimated in terms of $\mathbf{y} = (y^1, y^2) = (\dot{x}, \dot{y})$

¹²The quadratic form Q acts on the vertical fibre of velocities provided by the identification $T_{\dot{p}}\mathbb{R}^2 \equiv \mathbb{R}^2$, assuming the flagpole fixed, $\dot{p} = (.2, 1)$.

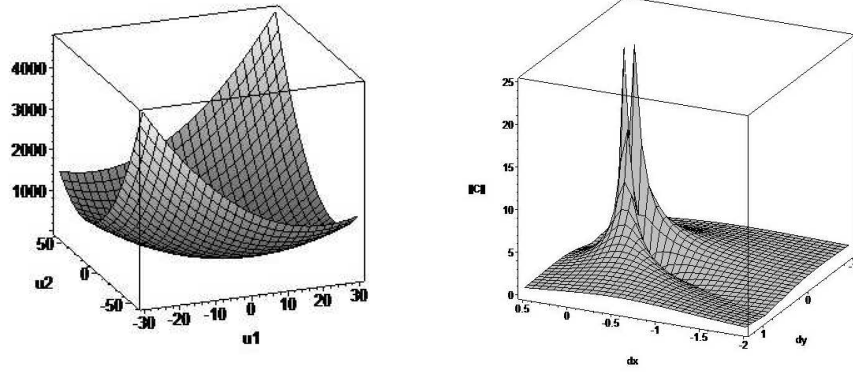


FIGURE 5. Graphs of the quadratic form Q_y^g and of $Q_y^C = \|C\|_y^2$ for $p \in [-1, 0.5] \times [-0.5, 1]$.

by the square of the Frobenius norm $Q_y^C = \|C\|_y^2$ (see Fig. 5), where

$$\|C\|_y = \sqrt{C_{ijk} g^{ir} g^{js} g^{kt} C_{rst}}.$$

The plot of the energy Q_y^C of C_{ijk} emphasizes a special region inside $[-1, 0.5] \times [-0.5, 1]$, at which the difference between the Randers norm and the canonic Euclidean norm significantly matter. This region (a small neighborhood of the origin) corresponds to slight variations of the cancer cell population, while for strong variations the Randers structure asymptotically approaches the canonic Euclidean one.

4.2. The induced Euclidean structures. The Euclidean case δ is canonic, hence the corresponding equations from Propositions 2.1 and 2.2 produce the constant conformally flat factor and the constant deviation angle,

$$\text{pr}_\delta g_E \approx 0.72\delta, \quad \theta_E \approx 0.71.$$

4.3. The 4-root type structure. For the 4-th root Finsler metric, the substitution of fit truncated parameters (3.11) into the corresponding equations of Propositions 2.1 and 2.2 produce the following

COROLLARY 4.2. *The conformally Euclidean projection of the metric produced by 4-root type Finsler structure (3.12) and the deviation angle between the metric and its δ -projection respectively are*

$$\text{pr}_\delta g_Q = \frac{1}{16F_Q^6} p \delta, \quad \theta_Q = \arccos \frac{p}{\sqrt{2s}},$$

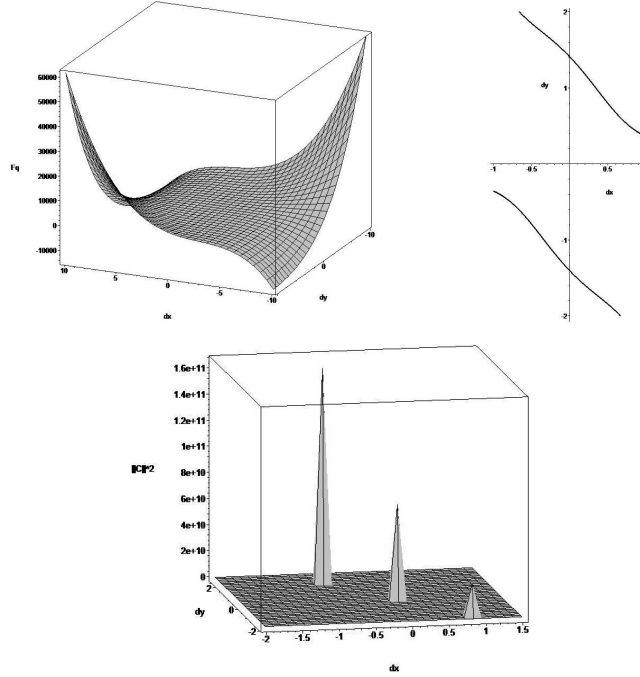


FIGURE 6. Graph of the energy $z = F^2(x, y)$, indicatrix $F_Q(x, y) = 1$ and squared Cartan norm $z = Q_y^C$ of the 4-th root Finsler structure

where

$$\begin{aligned}
 p &\approx 9.61x^6 + 14.93x^5y - 27.64x^4y^2 - 41.64x^3y^3 - 26.05x^2y^4 - 11.31xy^5 - 1.78y^6, \\
 s &\approx 1.83x^{12} - 1.34x^{11}y + 7.72x^{10}y^2 + 40.57x^9y^3 + 87.11x^8y^4 \\
 &\quad + 104.79x^7y^5 + 84.73x^6y^6 + 52.57x^5y^7 + 25.57x^4y^8 \\
 &\quad + 9.59x^3y^9 + 2.72x^2y^{10} + 0.49xy^{11} + 0.04y^{12}.
 \end{aligned}$$

The parameters of both type structures, F_R and F_Q have similar graphs, though the structures strongly differ, and the indicatrix of F_Q is nonconvex.

As well, the nature of F_Q causes much stronger dependency of the metric tensor on the directional argument, particularly in the neighborhood of $(0, 0)$ (see Fig. 6).

5. The relevance of the Finsler structures for the Garner model

We note that the fit Randers–Finsler norm (3.3) arises from the evaluation of the GS evolution-rate in terms of the reduced RS , and provides a mediated information on the prognosis of the disease after the state worsening signaled by the increase of the parameter h . The additive term $\beta = 0.63x - 0.27y$ from the Randers norm evaluates the impact of the change in the parameter h and the rate of increase.

The statistically determined coefficients $(b_1, b_2) \approx (0.63, -0.27)$ emphasize the dominant role of the proliferating cells in the dynamical system (1.1).

The Finsler norm (3.3) provides an evaluation of the severity of the rate of cancer cell evolution immediately after a significant change of the Garner parameter h , which can be experimentally measured or estimated in terms of the cause which determined the change.

The benefit of the Randers structure relies on the fact that the vector input $y = \dot{p}$ of F (the growth rates of the cancerous cells) does not require knowledge of the amount of the total cell populations p .

These inputs can be experimentally determined when the cancer evolution is controlled ("steady", for $h \approx 0$), and can be estimated by measuring the population increase/decrease of the cancerous cells by using only two subsequent laboratory samples.

Moreover, the deformation term $\beta = 0.63\dot{x} - 0.27\dot{y} \approx \|\dot{p}_e\| - \|\dot{p}\|$ represents the *drift*¹³ [7], which affects the straight paths of the Euclidean norm α , producing the new, curved paths of our Randers structure $F_R = \alpha + \beta$.

The Euclidean and the 4-th root fit Finsler norms exhibit different properties of the variation of cell populations. While F_E gives account via g_E on the anisotropic evolution of the illness process in the \dot{p} 2-dimensional plane through its PCA spectral data, the 4-th root norm $F_Q(\mathbf{y}) = \sqrt[4]{P_4(\mathbf{y})}$ is much more dense in information, through the larger spectral data of its $(0, 4)$ tensor induced by halvings by the 4-homogeneous in the components of the quadratic polynomial $P_4(\mathbf{y})$. The qualitative advantage over the Euclidean case is sensed within the space of 4-th root Finsler norms by the difference $\Delta(y) = \sqrt[4]{P_4(y)} - \sqrt[4]{F_E^2(y)}$.

6. Conclusions

A Finsler norm which fits the data provided by the Garner dynamical system is constructed. This leads to a Randers Finsler structure of locally Minkowski type, which mainly gives account of the changes of the Garner vector field, in terms of its parameters. The norm *provides a measure of the status change* of the cancer cell proliferation, related to a significant increase of the growth factor parameter h in the Garner system, which modifies its dynamics, and allows to fairly estimate the change of the variation rate based on laboratory subsequent samples.

As well, considerations on the conformally Euclidean projections of the three fit Finsler norms are produced, and the deviation from the canonic Euclidean framework are described by the angle formed by the conformally canonic Euclidean projection, computed within the Hilbert space of d -tensors, endowed by the canonic scalar product between tensors.

Further developments on the information provided by Finslerian norm (3.2) towards the original dynamical system are under current research, and will be presented in a forthcoming paper.

¹³In general, in terms of Zermelo navigation [9], the Randers structure represents the most appropriate model for exhibiting through its geodesics the influence of the β -force field on the geodesic trajectories of the Riemannian structure given by α .

Acknowledgement. The authors thank the transfusion medicine specialist Dr Zdravko Gulan from Blood Transfusion Institute of Vojvodina, for the valuable discussions and comments regarding the Garner model medical background.

References

1. P.L. Antonelli, I. Bucataru, *New results about the geometric invariants in KCC-theory*, An. St. Univ. "Al. I. Cuza" Iasi. Mat. N. S. **47** 2001, 405–420.
2. L. Astola, L. Florack, *Finsler Geometry on higher order tensor fields and applications to high angular resolution diffusion imaging*, Int. J. Comput. Vis. **92** 2011, 325–336. DOI 10.1007/S11263-010-0377-Z
3. V. Balan, I.R. Nicola, *Static bifurcation diagrams and the universal unfolding for cancer cell population model*, Proc. 9-th WSEAS Internat. Conf. on Mathematics and Computers in Biology and Chemistry (MCBC' 08), Bucharest, Romania, June 24–26, 2008.
4. ———, *Versal deformation and static bifurcation diagrams for the cancer cell population model*, Q. Appl. Math. **67**(4) 2009, 755–770.
5. ———, *Berwald-Moor metrics and structural stability of conformally-deformed geodesic SODE*, Appl. Sci. **11** 2009, 19–34.
6. D. Bao, S.-S. Chern, Z. Shen, *An Introduction to Riemann-Finsler Geometry*, Grad. Texts Math. 200, Springer-Verlag, 2000.
7. D. Bao, C. Robles, Z. Shen, *Zermelo navigation on Riemannian manifolds*, J. Differential Geom. **66**(3) 2004, 345–479; arXiv:math/0311233.
8. I. Bucataru, R. Miron, *Finsler-Lagrange geometry. Applications to dynamical systems*, Editura Academiei Romane, Bucuresti, 2007.
9. X. Cheng, Z. Shen, *Finsler Geometry: An approach via Randers Spaces*, Science Press and Springer, 2012.
10. S.-S. Chern, Z. Shen, *Riemann-Finsler Geometry*, World Scientific, 2005.
11. J.P. Freyer, R.M. Sutherland, *Regulation of growth saturation and development of necrosis in EMT6/R0 multicellular spheroids by the glucose and oxygen supply*, Cancer Res. **46** 1986, 3504–3512.
12. A.L. Garner, Y.Y. Lau, D.W. Jordan, M.D. Uhler, R.M. Gilgenbach, *Implication of a simple mathematical model to cancer cell population dynamics*, Cell Prolif. **39** 2006, 15–28.
13. A.M. Luciani, A. Rosi, P. Matarrese, G. Arancia, L. Guidoni, V. Viti, *Changes in cell volume and internal sodium concentration in HrLa cells during exponential growth and following Ionidamine treatment*, Eur. J. Cell Biol. **80** 2001, 187–195.
14. R. Miron, M. Anastasiei, *Vector Bundles and Lagrange Spaces with Applications to Relativity*, Geometry Balkan Press, Romania, 1997.
15. T. Reya, S.J. Morrison, M.F. Clarke, I.L. Weissman, *Stem cells, cancer, and cancer stem cells*, Nature **414** 2001, 105–111.
16. G.I. Solyanik, N.M. Berezetskaya, R.I. Bulkiewicz, G.I. Kulik, *Different growth patterns of a cancer cell population as a function of its starting growth characteristics: Analysis by mathematical modelling*, Cell Prolif. **28**(5) 1995, 263–278.

Department Mathematics-Informatics
 Faculty of Applied Sciences
 Univ. Politehnica of Bucharest
 Romania
 vladimir.balan@upb.ro

(Received 24 04 2014)
 (Revised 04 07 2014)

Technical Faculty "Mihajlo Pupin"
 University of Novi Sad
 Zrenjanin
 Serbia
 jelena@tfzr.uns.ac.rs